Automatic delineation of the osseous interface in ultrasound images by information fusion

Daanen Vincent
TIMC/GMCAO
IN3S
38706 La Tronche cedex
France
Vincent.Daanen@imag.fr

Tonetti Jerome
Orthopaedic Department
A. Michallon, University Hospital
38043 Grenoble
France
jtonetti@chu-grenoble.fr

Troccaz Jocelyne
TIMC/GMCAO
IN3S
38706 La Tronche cedex
France
Jocelyne.Troccaz@imag.fr

Abstract – *We present a new method for delineating the osseous interface in ultrasound images. Automatic segmentation of the bone-soft tissues interface is achieved by mimicking the reasoning of the expert in charge of the manual segmentation. Informations are modeled and fused by the use of fuzzy logic and the accurate delineation is then performed by using general a priori knowledge about osseous interface and ultrasound imaging physics. Results of the automatic segmentation are compared with the manual segmentation of an expert.*

Keywords: Ultrasound imaging, image processing, segmentation.

1 Introduction

In computer-aided surgery (CAS) such as orthopedic surgery, the knowledge of the bone volume position and geometry in the operative room is essential. The usual way to acquire this one is to register pre-operative data (i.e. acquired before the surgical operation) within per-operative data (i.e. acquired during the surgical operation, in the operating room).

For the last years, the use of ultrasound imaging as per-operative imaging has growned because investigations are inexpensive and riskless, and using 6D localized ultrasound probe, it's possible to reconstruct the 3D shape of a structure after its delineation ([1], [2], [3]).

Therefore, the extraction of structures from ultrasound data appears to be a delicate key point in CAS. Several methods have been proposed for achieve the delineation of features in ultrasound images : semi-automatic ([4], [5]), automatic [6],[7]) but these methods are always specific to a part of the human body because of the poor qualities of the ultrasound images, i.e. low contrast, low signal-to-noise ration and speckle noise of ultrasound images.

We propose a fully automated method for the delineation of the bone-soft tissues interface in ultrasound images based on information fusion : data available in images are modeled and fused by the use of fuzzy logic. We then mimic the expert's reasoning to accurately delineate the osseous interface.

2 MATERIAL AND METHOD

2.1 Material

Ultrasound imaging is achieved by using a US probe which is localized in 3D space by an optical localizer. The US probe is calibrated according to the technique described in [8]. This allows us to compute the position of an image pixel in 3D space with a precision in the range of the optical localizer and thus the shape of an organ [9].

2.2 Method

In this section, we introduce the expert's reasoning and the way we mimic it in order to achieve an accurate segmentation of the osseous interface.

2.2.1 Expert's reasoning

The expert's reasoning is based on one hand on the physical of the ultrasound imaging and on the other hand on his knowledge in anatomy. Ultrasound imaging enhances the interfaces between anatomical structures and amplitudes of the US echos depend on the difference between acoustical impedances of successive tissue layers. In the case of bone imaging, the great difference of acoustical impedance between the bone and its surrounding tissues generates an important echo and because bones have a high absorption rate there is no imaging possible beyond them (shadow effect) ; therefore the expert pays attention to *bright* pixels followed by a globally dark area. The expert also uses its knowledge of anatomy and selects pixels whose are belonging to a continuous curve (i.e. which does not present discontinuities such as 'jump') among which one the contrast is high and homogeneous.

We propose a method that mimics the reasoning of the expert. The method is divided into 3 steps :

- the *fuzzy processing* step,
- the 'continuity-ness' cost function computation step,
- the contrast computation and decision making.

2.2.2 Fuzzy Process

The aim of the fuzzy process step aims is to model the information available in the images and then concentrate them into one image representing the membership of the pixel to a given property.

Fuzzy Intensity Image : In ultrasound imaging, bones appear to be hyper-echoic because of the difference of acoustical impedance, therefore *bright* pixels constitute an indication of the location of the osseous interface, but is not an

absolute criteria. Consequently, the fuzzification function have to give an important (resp low) membership value to *bright* (resp *dark*) pixels. In a previous development [10], we point out that binarizing the initial ultrasound image in regard of the Otsu's threshold (T_{Otsu})[11], gives a good approximation of the echogenic area and so, of the position of the osseous interface. The computation of the Otsu's threshold requires the computation of a criterion (we call V_{Otsu}) which measures the separability of the *foreground* and *object* classes (see [11] for details) ; we make use of this criterion to build the fuzzification function $\mu_{_{Int}}$ as follows : first, V_{Otsu}, associated to the image currently processed, is normalized and cumulated. Then, this curve is shifted in order to force the membership function value

$$\mu_{_{Int}}(T_{_{Otsu}}) = 0.5, \tag{1}$$

Processing this way, the fuzzification function is closed to the well-known S-function. Finally, we apply the fuzzification function over the gray-level image in order to achieve the construction of the fuzzy intensity image $FII(p)$ which gives for a pixel p of the intensity image its membership degree to the echogenic area.
Fig. 1 shows 2 ultrasound images we use to illustrate the method.

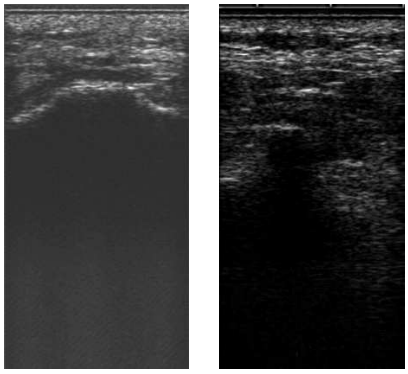

(a) (b)

Fig. 1: Original ultrasound images

Fig. 2 shows the intensity fuzzification function computed from the Otsu's criterion (Fig. 2-a and 2-c) and the Intensity Fuzzy Image (Fig. 2-b and 4-d).

Fuzzy Gradient Image : The gradient information constitutes another important part in the determination of the osseous interface and so the fuzzy gradient image $FGI(p)$ is of great interest. Indeed, the transition from the bone to the acoustic shadow area suggests to search for highly contrasted pixels and because ultrasound imaging should only 'detect' structure changes which are perpendicular to the ultrasound beam, we have to pay attention only to horizontal (or near horizontal) edges, therefore we use a 5x5 'horizontal-direction' MDIF edge detector (Equ 2).

$$\mathbf{F} = \begin{pmatrix} 0 & -1 & -1 & -1 & 0 \\ -1 & -2 & -3 & -2 & -1 \\ 0 & 0 & 0 & 0 & 0 \\ 1 & 2 & 3 & 2 & 1 \\ 0 & 1 & 1 & 1 & 0 \end{pmatrix} \tag{2}$$

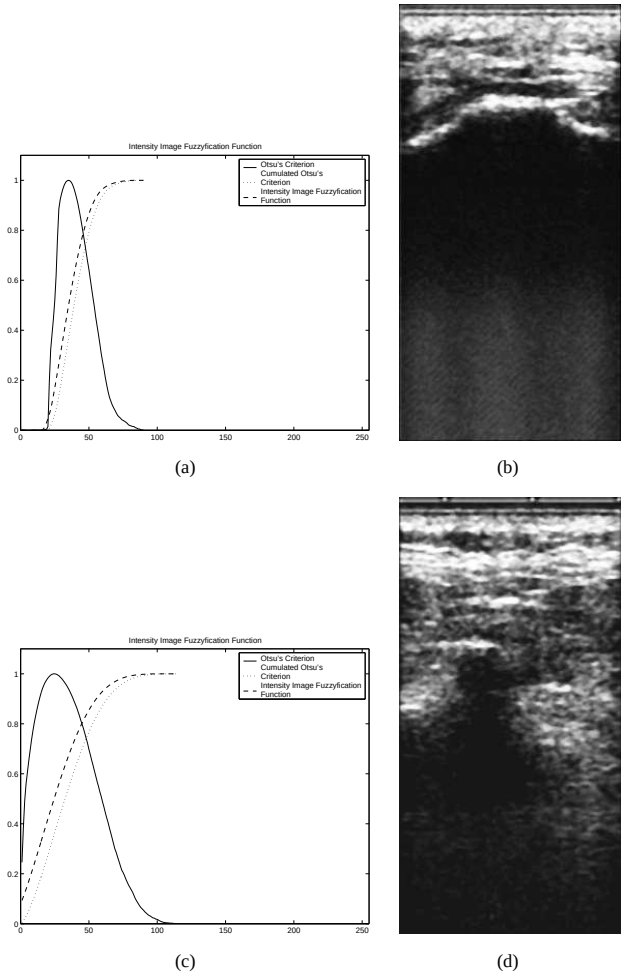

Fig. 2-a and 2-b refer to Fig. 1-a
and Fig. 2-c and 2-d refer to Fig. 1-b

Fig. 2: Computation of FII from the original ultrasound image

Edge detection using the MDIF detector may results in negative value, depending on the graylevel transition. In our case, we want to detect *bright-to-dark* transition. Therefore, we threshold the image resulting of the edge detection in order to remove the *dark-to-bright* transition. Finally, we use the well-known S-shape function (3) to perform the *fuzzification* of the gradient image and obtain the *Fuzzy Image Gradient* $FGI(p)$. The parameters a,b,c of the S-shape function are computed so that $S(x; a, b, c)$ is the closest s-shape function of the normalized cumulative histogram.

$$\begin{array}{rcll} S_{(x;a,b,c)} & = & 0 & \text{for } x < a \\ & = & \frac{(x-a)^2}{(b-a)(c-a)} & \text{for } a \leq x \leq b \\ & = & 1 - \frac{(x-c)^2}{(c-a)(c-b)} & \text{for } b \leq x \leq c \\ & = & 1 & \text{for } x > c \end{array} \tag{3}$$

One can see the gradient image (Fig. 3-a resp(3-c)) of Fig. 1-a (resp Fig. 1-b) and the Fuzzy Gradient Image (Fig. 3-b, (resp Fig. 3-d)).

Data Fusion : The data fusion step aims at concentrating all the information in order to produce a single membership value for each pixel of the analyzed image to the

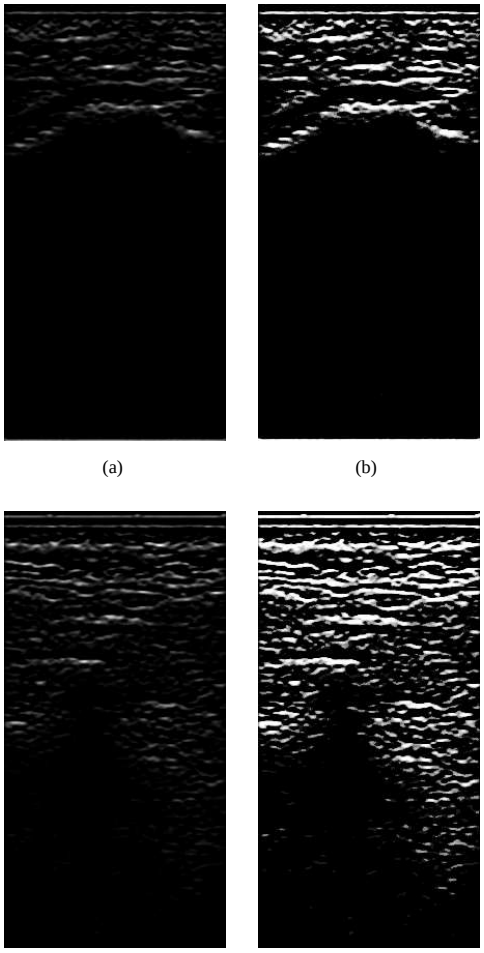

(a) (b)

(c) (d)

Fig. 3-a and 3-b refer to Fig. 1-a
and Fig. 3-c and 3-d refer to Fig. 1-b

Fig. 3: Gradient and Fuzzy Gradient Images

osseous interface. For our purpose, a pixel may belong to the osseous interface if both its gray-level and gradient are 'high'. Consequently, the fuzzy operator must 'detect' simultaneous satisfaction of criteria and 'reject' others cases. This combination is naturally achieved by a 'conjunctive-type' combination operator. We choose the simple fuzzy intersection operator *min* ; therefore the membership of a pixel to the osseous interface is given by :

$$FI_G(p) = min(FII(p), FGI(p)) \quad (4)$$

$FI_G(p)$ (Fig. 4) denotes the global degree of membership of the pixel *p* to the echogenic area and to an highly contrasted image area.

Defuzzification at a given membership degree μ : The defuzzification process aims at extracting from the fuzzy image $FI_(p)$ the osseous interface related to a membership degree μ_{ref}. To achieve this task, we make use of a priori knowledge about the physical of ultrasound imaging. As mentioned earlier, bones 'stop' the US-waves. In our purpose, this means that, for a column of the image, the pixel of the osseous interface related to a membership value μ_{ref} is the last (from the top) pixel which has a membership equal to μ_{ref}. At the end of this *defuzzification* process, at the most one pixel per column is highlighted. The 'curve' described by these pixels is called *profile* in the rest of the paper.

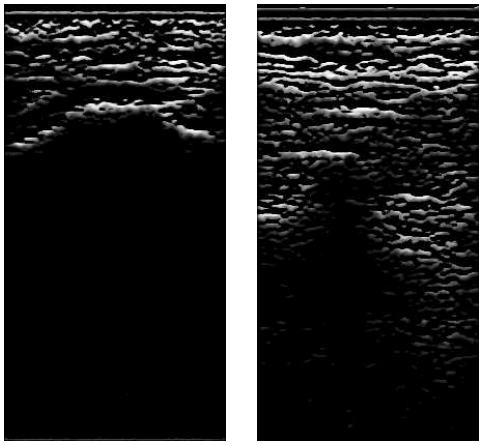

(a) (b)

Fig. 4-a refers to Fig. 1-a
and Fig. 4-b refers to Fig. 1-b

Fig. 4: Fuzzy Image

2.2.3 Computation of the optimal defuzzification threshold

In regards to the expert's reasoning, the optimal threshold described a continuous interface where the local contrast is maximum and homogeneous. Therefore, for each membership degree $0 < \mu < 1$ (μ space is discretized with a step $\delta_\mu = 0.005$), the deffuzzification of $FI_G(p)$ is performed and the 'continuity-ness' of the profile is evaluated. We then choose the membership degree which maximize the local contrast and the homogeneity of this one.

Evaluation of the 'continuity-ness' of the profile : As we mentioned earlier, actual osseous interfaces do not present discontinuities and therefore, the osseous interface we detect should be as smooth as possible. We use this property to determine the optimal defuzzification threshold by computing a 'cost function' that reflects the 'continuity-ness' of an computed osseous interface.
Because osseous interfaces may present several different shapes whose we do not have knowledge, we make use of the wavelet transform to evaluate the amount of discontinuities in the profile. Applying the wavelet transform (Discrete Wavelet Transform in our case) to a signal decomposes this one with a multiresolution scale factor of two providing at each resolution level one low-resolution approximation (A) and one wavelet detail (D) [12]. Experimentally, we choose the Daubechies-4 wavelet basis (several others basis have been tested and no dependence was pointed out at the exception of the Haar Basis) ; and the wavelet decomposition of the profile is performed twice. To reject small interfaces (4/5 pixels) detected when the membership value used for the defuzzification is unsuitable (i.e. when it is too high), we add a penalization term related to the length of the profile (Pen). The 'amount' of discontinuities in the profile is computed as follows :

$$\varepsilon(\mu) = E(D_1) + E(D_2) + Pen \quad (5)$$

Finally, $\varepsilon(\mu)$ is normalized and we compute the 'continuity-ness' of the profile as :

$$C(\mu) = 1 - \varepsilon(\mu) \tag{6}$$

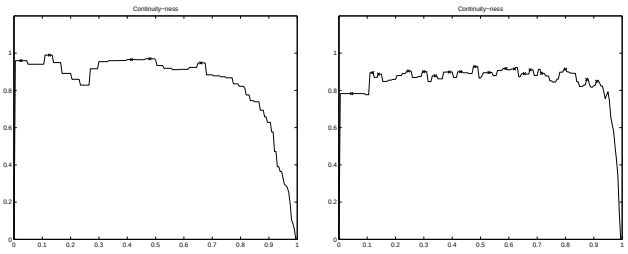

(a) (b)

Fig. 5-a refers to Fig. 1-a
and Fig. 5-b refers to Fig. 1-b

Fig. 5: continuity-ness' objective function

As one can see (Fig. 5), the 'continuity-ness' function $C(\mu)$ presents several local maxima (crosses on the curve : 5 and 18 in these cases). Each of them locates a membership degree μ where the associated profile is more continuous than the profiles of its neighbors and so each of them may be the optimal defuzzification threshold and therefore, we have to detect all of them. This detection is achieved by computing the watershed transform of $C(\mu)$. For each local maxima, the image is defuzzed to the corresponding membership degree μ and the local contrast is computed.

Local contrast computation : For each pixel *p* belonging to a profile, the local contrast $LC(p)$ associated to the pixel *p* is computed by :

$$LC(p) = \frac{\overline{Up} - \overline{Down}}{\overline{Up} + \overline{Down}} \tag{7}$$

where $\overline{Up}$ (resp $\overline{Down}$) is the mean value of the above (resp underneath) *roi*. This definition of the local contrast gives us a way to determine whenever the pixel *p* is in the vicinity of the osseous interface because the bone appears in the image as a 'light' area followed by a 'dark' area i.e. a positive local contrast. We obtain a cost function $Contrast(\mu)$ related to the global contrast along the profile and defined by :

$$Contrast(\mu) = \sum_{p} LC(p) \tag{8}$$

where p is the pixels of a profile.
We also expect that the contrast along the profile is homogeneous, therefore we also compute a measure of the homogeneity of the contrast along the profile. This is achieved by computing the standard deviation of the values of the contrast along the profile ([13] uses this criterion as a homogeneity measure) giving us a function $StdDev(\mu)$.

Optimal defuzzification threshold determination : The two cost-functions : $Contrast(\mu)$ and $StdDev(\mu)$ allow us to determine the optimal defuzzification threshold which maximizes the local contrast and the homogeneity of the values of contrast along the profile. This is achieved by computing the objective function :

$$Cost(\mu) = Contrast(\mu) + \frac{1}{StdDev(\mu)} \tag{9}$$

Finally, the optimal membership degree is the one that maximized $Cost(\mu)$:

$$\mu_{Optimal} = \arg max(Cost(\mu)) \tag{10}$$

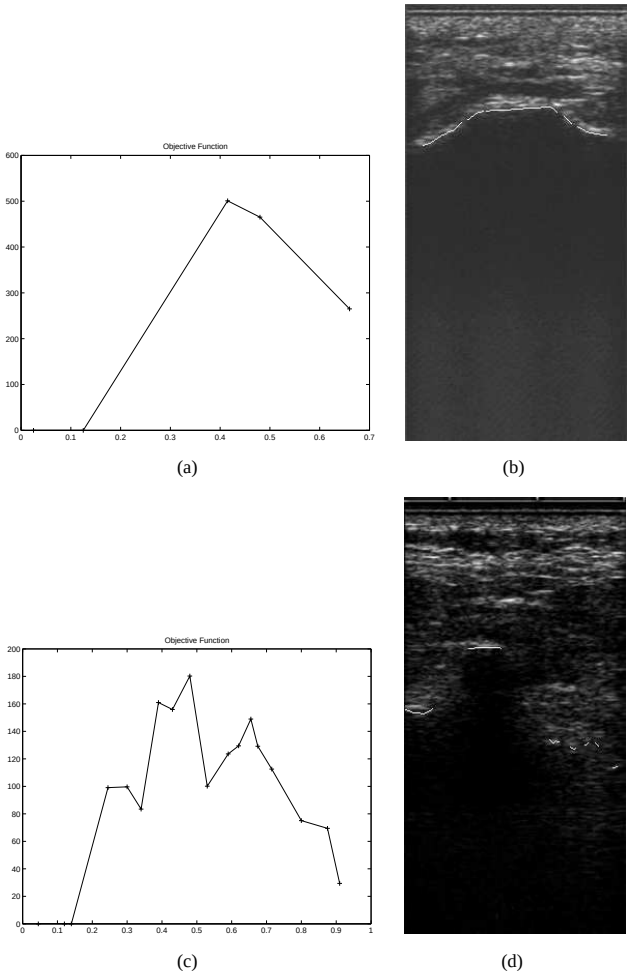

(a) (b)

(c) (d)

Fig. 6-a and Fig. 6-b refer to Fig. 1-a
and Fig. 5-c and Fig. 6-d refer to Fig. 1-b

Fig. 6: Objective function and resulting segmentation

Fig. 6-a (resp 6-c) shows the objective function computed by (9). Although the objective function may present several local maxima, choosing the global maximum results in a correct delineation as one can see in Fig. 6-b (resp 6-d)

3 RESULTS

Sacral ultrasound images segmentation: The images are acquired with a US-probe of 25 mm long working at a frequency of 7.5 MHz. The probe is calibrated and the pixel size is about 0.1mm x 0.1mm. An image of interest is extracted as a 214 x 422 sub-image from the 640 x 480 original images before being processed.

The proposed method have been tested on ultrasound images of sacrum coming from cadaver datasets [3] or patient datasets [14] : about 250 images have been processed. For each image, the manual segmentation of the expert is available and constitutes our gold-standard. For each image within a dataset, we compute the error between the manual segmentation and the segmentation computed by our method. We then compute the mean error for each image (Table 1-column 1) and the Haudorff distance (maximum over all errors within a subset) and mean absolute distance (average of all the maximum errors within a subset) (Table 1-column 2).

In order to evaluate the ability of the proposed method to delineate the osseous interface in strongly corrupted images, we also compute the Signal-to-mse ratio [15] (using a 5x5 median filter to denoise the image) which corresponds to the classical Signal-to-Noise ration computed in case of additive noise (Table 1-column 3).

Dataset	Segmentation Error mean/SD (pixel)	Max Errors mean/max (pixel)	S/mse mean/SD (dB)
Patient 1 (51 images)	7.808 / 1.995	12.137 / 22	5.052 / 0.185
Patient 2 (49 images)	8.807 / 3.177	16.905 / 25	5.206 / 0.428
Patient 3 (69 images)	4.545 / 3.874	17.0789 / 35	8.905 / 0.283
Cadaver 1 (37 images)	3.495 / 1.931	9.830 / 36	8.786 / 0.340
Cadaver 2 (41 images)	2.679 / 1.456	7.294 / 19	9.019 / 0.259
Cadaver 3 (39 images)	4.056 / 3.213	12.14 / 38	7.984 / 0.177

pixel size is 0.1mm.1mm

Table 1: segmentation errors

As one can see (Table 1) :

- the mean error of segmentation is always less than 10 pixels (i.e 1mm) even on highly corrupted images. However, it is clear that the accuracy of the delineation is correlated within the amount of noise and therefore, we think that taking into account the noise (measured by the S/sme ratio by example) during the fusion and/or delineation process may be a way to improve the delineation.
- the maximum errors still remain important but, according to us, it is not the error we should focus on : we point out that these errors occur at more or less one pixel on complex shapes(such as medial sacral crest or sacral hiatus) giving thus an important maximum error in regards to the manual delineation but the overall error on the global shape still remains negligible.

Vertebra ultrasound images segmentation: The method was used for the delineation of the osseous interface in vertebrae images. We acquired 42 images of the L4 vertebra in several orientation, we use a linear probe working a 7.5 MHz of 80 mm long. The pixel size is about 0.182mm x 0.178mm. For each image, we extract the image of interest (346x467 pixels) from the 768x576 original image.

Once the segmentation process achieved, we convert the result in a 3D points cloud (remember that the US-probe is calibrated). The results were validated by the expert, the validation is based on the visual resemblance of the 3D points cloud within the 'imaged' bone.

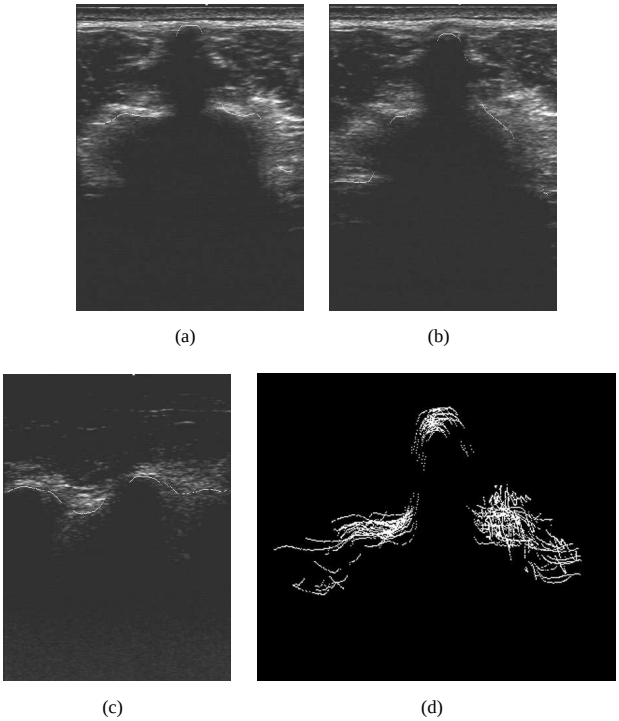

(a) (b) (c) (d)

Fig. 7: Delineation of the osseous interface of ultrasound images of vertebrae

Fig. 7 shows some ultrasound images with the computed delineation : Fig. 7-a and Fig. 7-b show the delineation of the spinous process of the vertebra (referred as 1 on Fig. 8) and Fig. 7-c shows the delineation of the osseous interface in an image taken in the area referred as 2 on Fig. 8[1]. The 3D points cloud computed from the delineations is shown in Fig. 7-d. One can clearly recognize the spinous process which the feature of interest in CAS of the vertebrae because its shape is of great help during the registration process.

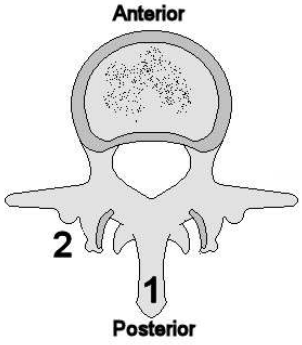

(a)

Fig. 8: a lombar vertebra

[1] explanations on the imaging of a vertebra with ultrasound can be found in [6]

4 DISCUSSION

We presented a method dedicated to the delineation of the osseous interface in ultrasound images. This method, based on fusion information, mimics the expert's reasoning and models several a priori knowledges source to achieve the delineation.

It is of broad importance to point out that our method have been tested on images from cadavers but also on images from patients. As one can see (column 3 of table 1), images of patients appears to be noisier than cadaver images and in all cases, we obtain a quite accurate delineation.

The proposed method have been found to be 'independent' of the overall shape of the osseous interface : several shapes were present in the images we segmented with the proposed method and in every case, the correct osseous interface was delineated. The method appears to be a generic method for he delineation of the osseous interface in linear ultrasound images. For sectorial images, a small part of the process (the part described in the paragraph *Defuzzification at a given membership degree* μ) should be modified to take int account the particularity of a sectorial probe.

At present, our validation is based on a comparison of the result of the automated segmentation process within the manual delineation of the osseous interface by an expert. Even if the expert pays attention to the work, we can not exclude that some errors occur : on some image, the expert abstains to delineate any osseous interface whereas the presented method find one with no ambiguity. In order to suppress any doubt about the position of the osseous interface, we will soon start a validation based on the comparison of the rigid registration of the dataset obtained by the proposed method within a dataset obtained by the direct palpation of the bone surface within a localized probe pointer as described in [16].

5 CONCLUSION

In this paper, we presented a method for automatic delineation of the osseous interface in ultrasound image. The method is based on information fusion and it mimics the expert's reasoning. The method has been found to be accurate and fast enough to be used in per-operative step of computer aided surgeries. The method have been used to delineate osseous interface in ultrasound images of the sacrum which may present several shapes and good results were obtained and we think that the described method a first step toward robust delineation of the osseous interface in ultrasound images.

Acknowledgements

This work has been partly supported by the french research project RNTS 'Surgetique'.

References

[1] O. Schorr and H. Wrn. A New Concept for Intraoperative Matching of 3D Ultrasound and CT. In *Proceedings of MMVR : Medecine Meets Virtual Reality*, pages 446–452, 2001.

[2] O. Krivonos, J. Hesser, R. Mnner, F. Gebhard, U. Liener, P.Keppler, and L.Kinzl. Minimal Invasive Surgery of the Pelvis using Ultrasound. In *4^{th} CAOSUSA Conference in Pittsburg, Pensylvannia*, pages 203–205, 2000.

[3] L. Carrat, J.Tonetti, S. Lavallée, Ph. Merloz, L. Pittet, and JP. Chirosset. Treatment of Pelvic Ring Fractures : Percutaneous Computer Assisted Iliosacral Screwing. In *CS Serie, Springer Verlag, MICCAI*, volume 1496, pages 84–91, 1998.

[4] A. Krivanek and M. Sonka. Ovarian Ultrasound Image Analysis : Follicle Segmentation. *IEEE Transactions on Medical Imaging*, 17(6):935–944, 1998.

[5] SD. Pathak, DR. Haynor, and Y. Kim. Edge-Guided Boundary Delineation in Prostate Ultrasound Images. *IEEE Transactions on Medical Imaging*, 19(12):1211–1219, 2000.

[6] B. Brendel, S. Winter, A. Rick, M. Stockheim, and H. Ermert. Registration of 3D CT and Ultrasound Datasets of the Spine using Bone Structures. *Computer Aided Surgery*, 7(3):146–155, 2002.

[7] D.V. Amin, T Kanade, A.M. DiGioia III, and B. Jaramaz. Ultrasound Registration of the Bone Surface for Surgical Navigation. *Computer Aided Surgery*, (8):1–16, 2003.

[8] T. Lang. *Ultrasound Guided Surgery : Image Processing and Navigation*. PhD thesis, Norwegian University of Science and Technology, Trondheim, Norway, 2000.

[9] C. Barbe, J. Troccaz, B. Mazier, and S. Lavallée. Using 2.5D Echography in Computer Assisted Spine Surgery. In *Proceedings of the 15^{th} Annual International Conference of the IEEE Engineering in Medicine and Biology Society*, pages 160–161, 1993.

[10] V.Daanen, J.Tonetti, J. Troccaz, and Ph. Merloz. Automatic Determination of the Bone-Soft Tissues Interface in Ultrasound Images. First Results in Iliosacral Screwing Surgery. In *Proceedings of Surgetica-CAMI 2002*, pages 144–151, 2002.

[11] N. Otsu. A Threshold selection Method from Gray-Level Histograms. *IEEE Transactions on Systems, Man, and Cybernetics*, 9(1):62–66, 1979.

[12] S. Mallat and WL. Hwang. Singularities Detection and Processing with Wavelets. *IEEE Transactions on Information Theory*, 32(2), 1992.

[13] M. Garza, P. Meer, and V. Medina. Robust Retrieval of 3D Structures from Image Stacks. *Medical Image Analysis*, 3(1):21–35, 1999.

[14] L. Carrat, J.Tonetti, Ph. Merloz, and J. Troccaz. Percutaneous Computer Assisted Iliosacral Screwing : Clinical Validation. In *CS Serie, Springer Verlag, MICCAI*, volume 1679, pages 1229–1237, 2000.

[15] A. Achim, A. Bezerianos, and P. Tsakalides. Novel Bayesian Multiscale Method for Speckle Removal in Medical Ultrasound Images. *IEEE Transactions on Medical Imaging*, 20(8):772–783, 2001.

[16] G. Ionescu, S.Lavallée, and J. Demongeot. Automated Registration of Ultrasound with CT Images : Application to Computer Assisted Prostate Radiotherapy and Orthopedics. In *CS Serie, Springer Verlag, MICCAI*, volume 1679, pages 768–777, 1999.